Cascade of torus birth bifurcations and inverse cascade of Shilnikov attractors merging at the threshold of hyperchaos

I. R. Sataev[1] and N.V. Stankevich[2]
[1)]*Kotelnikov Institute of Radioengineering and Electronics of RAS, Saratov Branch, 410019, Zelenaya str., 38, Saratov, Russia*[a)]
[2)]*National Research University Higher School of Economics, Bolshaya Pecherskaya str., 25/12, Nizhny Novgorod, 603155, Russia*[b)]

(Dated: 20 January 2021)

We study the hyperchaos formation scenario in the modified Anishchenko-Astakhov generator. Scenario is connected with the existence of sequence of secondary torus bifurcations of resonant cycles preceding the hyperchaos emergence. This bifurcation cascade leads to the birth of the hierarchy of saddle-focus cycles with two-dimensional unstable manifold as well as of saddle hyperchaotic sets resulting from the period-doubling cascades of unstable resonant cycles. Hyperchaos is born as a result of an inverse cascade of bifurcations of the emergence of discrete spiral Shilnikov attractors, accompanied by absorbing the cycles constituting this hierarchy.

The scenario of the birth of a hyperchaotic attractor is closely related to the scenario of the emergence of an infinite set of cycles with a multi-dimensional unstable manifold making up its skeleton. For four-dimensional flows there are not so many local bifurcations leading to the birth of a cycle with a two-dimensional unstable manifold - these are the torus bifurcation (often called Neimark-Sacker bifurcation) of the stable cycle and the period-doubling bifurcation of the saddle cycle. The birth of such a cycle as a result of a saddle-node bifurcation is also possible, but this is not our case. The case under consideration is interesting in that the two of the three possibilities are involved. The cascade of creation of secondary tori from stable resonance cycles leads to the appearance of the hierarchy of saddle-foci arising as a result of Neimark-Sacker bifurcations. At each stage of this cascade, saddle resonance cycle appear, which undergoes a cascade of period-doubling bifurcations. On the one hand the absorption of these cycles by the attractor ultimately leads to the appearance of hyperchaos. On the other hand this inverse cascade of bifurcations of cycle absorbing is accompanied by the emergence of discrete spiral Shilnikov attractors. Discrete spiral Shilnikov attractors were discovered in 1986. The term "hyperchaos" was introduced first in 1979. Both events happened almost together but it took more than 30 years to combine them in the one universal scenario. The existence of a large number of examples in which the birth of hyperchaos is associated with the existence of secondary torus birth bifurcations and the occurrence of discrete spiral Shilnikov attractors indicates the prevalence of this scenario.

I. INTRODUCTION

Hyperchaos[1] is a dynamic regime characterized by at least two positive Lyapunov exponents, that is, there are at least two directions of extension in the phase space. Attractor of this type can be implemented in flow systems with a dimension of at least 4.

Chaos-hyperchaos transition scenarios usually refer to one of two types: either trajectories belonging to a chaotic attractor lose stability in one more direction, or the attractor absorbs an infinite number of trajectories with a two-dimensional unstable manifold[2–9].

If orbits with a two-dimensional unstable manifold arise as a result of the Neimark-Sacker bifurcation, then one of the typical scenarios of their capture by an attractor is the appearance of so-called discrete spiral Shilnikov attractors[10–13]. Such attractors have been found in 3D maps. They can also occur in flow systems of dimension 4 and higher.

We consider here an example of a system in which cycles with a two-dimensional unstable manifold arise as a result of a cascade of Neimark-Sacker bifurcations (this results in a set of saddle-foci of type (1,2)) and of cascades of period-doubling of saddle resonance cycles near the transition to hyperchaos. (The type of cycle is indicated here by a pair of numbers in brackets, the first is the dimension of a stable manifold, the second - of an unstable one.) In this case, hyperchaos is born as a result of an inverse cascade of bifurcations of the emergence and merging of discrete spiral Shilnikov attractors.

The paper is structured as follows. In Section II, we briefly describe the object of research - the modified Anishchenko-Astakhov generator, define and illustrate the regions of interest to us in the parameter space. In Section III, we describe the bifurcation structure of the period four synchronization tongue. In Section IV, we will demonstrate a cascade of secondary Neimark-Sacker bifurcations, which results in the formation of a hierarchy of saddle-focus cycles of type (1,2). In Section V, we will demonstrate cascades of period-doubling bifurcations of the saddle resonance cycles (of type (2,1)), which results in the formation of a hierarchy of sets of saddle cycles (of type (1,2)). In Section VI, we will demonstrate the inverse cascade of the emergence of discrete spiral hyper-

[a)]Electronic mail: sataevir@gmail.com
[b)]Also at Yuri Gagarin State Technical University of Saratov, Politehnicheskaya str., 77, Saratov, 410054, Russia; Also at St.Petersburg State University, Universitetskiy proezd, 28, Peterhof, Saint-Petersburg, 198504, Russia; Electronic mail: stankevichnv@mail.ru

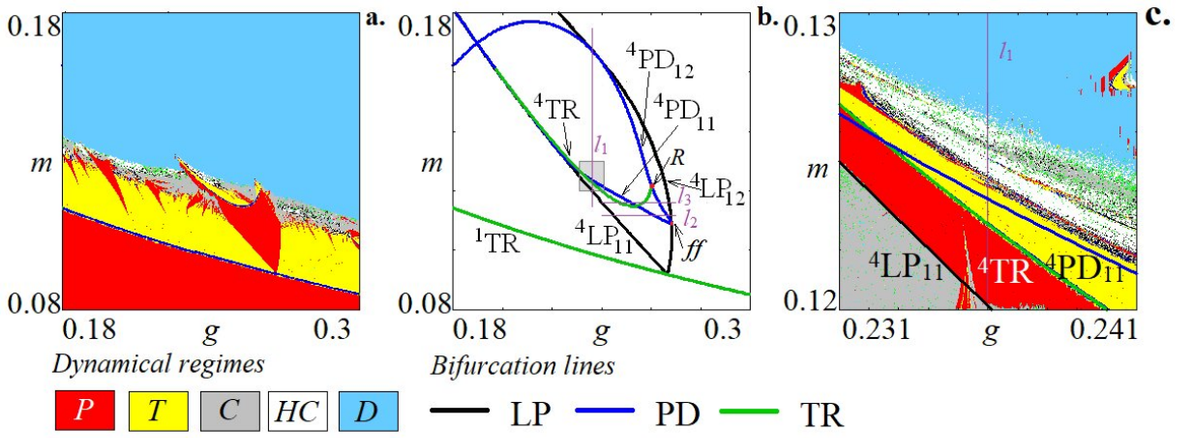

FIG. 1. Lyapunov exponents chart, **a.** and two-parameter bifurcation diagram, **b.** for the system (1) at d=0.001, $\gamma = 0.2$. **c.** Zoomed fragment of Lyapunov exponents chart correspoding to the gray rectangle in Fig. 1b. LP are lines of the saddle-node bifurcations (black), PD are lines of the period-doubling bifurcations (blue), TR are lines of the Neimark-Sacker bifurcation (green). Line l_1 corresponds to $g = 0.236$, l_2, l_3 - to $m = 0.112$, $m = 0.115$, respectively.

chaotic attractors as a result of the gradual absorption of saddle cycles (1,2). Section VII will give final conclusions and discussion about the universality of the observed bifurcations and scenario.

II. MODIFIED ANISCHENKO-ASTAKHOV GENERATOR

In[14,15], an autonomous four-dimensional dynamic system is proposed, which is a radiophysical generator:

$$\begin{aligned} \dot{x} &= mx + y - x\varphi - dx^3, \\ \dot{y} &= -x, \\ \dot{z} &= \varphi, \\ \dot{\varphi} &= -\gamma\varphi + \gamma\Phi(x) - gz. \end{aligned} \tag{1}$$

where $\Phi(x) = I(x)x^2$, $\quad I(x) = \begin{cases} 1, & x > 0, \\ 0, & x \le 0 \end{cases}$.

Here x, y, z, ϕ are the dynamic variables of the system, m is the excitation parameter, d is the nonlinear dissipation parameter, γ is the damping parameter, and g is the inertia parameter.

Fig. 1a shows chart of Lyapunov exponents for system (1) on the parameter plane (g, m). The values of the remaining parameters are $d = 0.001$, $\gamma = 0.2$. The chart was constructed in the following way: the plane of parameters is covered by a grid of nodes; for each node, the spectrum of Lyapunov exponents was calculated. Depending on the spectrum signature, a point on the parameter plane was colored in one color or another in accordance with the palette shown in the figure (Table I shows the signature of the modes). Fig. 1b shows two-parametric bifurcation diagram obtained using the package for numerical bifurcation analysis XPPAUT[16]. The lines of saddle-node bifurcations (LP) are shown in black, the lines of period-doubling bifurcations (PD) are shown in blue, and the lines of Neimark-Saker bifurcations (TR) are shown in green. In Fig. 1c a zoomed fragment of the chart is presented corresponding to grey rectangle in Fig. 1b.

Mode	***Signature***	Color
Periodic	$\Lambda_1 = 0, \Lambda_4 < \Lambda_3 < \Lambda_2 < 0$	Red
Torus	$\Lambda_1 = \Lambda_2 = 0, \Lambda_4 < \Lambda_3 < 0$	Yellow
Chaotic	$\Lambda_1 > 0$, $\Lambda_2 = 0, \Lambda_4 < \Lambda_3 < 0$	Grey
Hyperchaotic	$\Lambda_1 \ge \Lambda_2 > 0$, $\Lambda_3 = 0$, $\Lambda_4 < 0$	White
div	The trajectory goes to infinity	Blue

TABLE I. Correspondence of Lyapunov spectrum signature and color designation of modes for Lyapunov exponent chart

The lower part of the plane of parameters (Fig. 1a) is occupied by the region of existence of a stable cycle of period-1. The period of the cycle was determined by the number of intersections of the trajectory of the system with the plane of the Poincaré section y = 0. As the parameter m increases, the cycle of period-1 undergoes a Neimark-Sacker bifurcation with the creation of an invariant circle in the Poincaré section. In Fig. 1b this bifurcation line is denoted by symbol ^{1}TR, here and further upper index before bifurcation symbol designates the period of the cycle which undergoes bifurcation. Fig. 1a clearly shows regions of periodic regimes, which lies in the domain of quasiperiodicity. It is a set of Arnold tongues (which are also called synchronization tongues) with different ratio of frequencies located along torus birth bifurcation line. The vastest region is a period four Arnold tongue. With increasing parameter m we can observe the destruction of a closed invariant curve via the Afraimovich-Shilnikov scenario[17]. Further increasing of parameter m leads to regime of divergency, when phase trajectories go to infinity. Inside Arnold tongue of period 4 (magnified part of which is shown in the Fig. 1c) we can see a narrow domain of of hyperchaotic regimes. Let us discuss in more detail the bifurcation diagram presented in Fig. 1b which defines the structure of this tongue.

III. PERIOD FOUR ARNOLD TONGUE

Fig. 1b presents two-parametric bifurcation diagram, where we focus on the bifurcation lines forming period-4 Arnold tongue and development of complex behavior inside it. As usual the boundaries of Arnold tongue are formed by two saddle-node bifurcation lines, (^{4}LP$_{11}$ and ^{4}LP$_{12}$), emerging from the point located at the Neimark-Sacker bifurcation line. As a result of saddle-node bifurcation a pair of period four cycles appears, stable and unstable one. Inside the tongue unstable cycle undergoes period-doubling bifurcation, the corresponding bifurcation line is denoted in the figure as ^{4}PD$_{11}$. The stable cycle may also undergo period-doubling bifurcation (^{4}PD$_{12}$ line) near the right border of the tongue, but in the left part of the diagram it changes for Neimark-Sacker bifurcation (^{4}TR line). This two lines intersect at the codimension-2 resonance 1:2 point, denoted by symbol R. In Fig. 1b with symbol ff we denote another codimension-2 point where saddle-node and period-doubling bifurcation lines touch. This is so called fold-flip point[27] . Below this point as a result of saddle-node bifurcation a pair of stable and saddle cycles is born. Above this point both cycles in pair are saddles, but they have different dimensions of unstable and stable manifolds.

Fig. 2 shows three one-parameter bifurcation diagrams for the simplest period 4 resonance cycle. In these diagrams, we marked cycles of various types with three colors: green - stable limit cycles P(3,0), blue - cycles with one-dimensional unstable manifold S(2,1), and orange - cycles with two-dimensional unstable manifold S(1,2). We chose two directions of scanning the parameter plane: varying the parameter m (Fig. 2a) and g (Fig. 2b, 2c). In Fig. 1b we have marked corresponding routs by violet lines l_1, l_2, l_3.

Along line l_1 in Fig. 2b we fix $g = 0.236$. At $m = 0.1201$, as a result of the saddle-node bifurcation (marked as ^{4}LP$_{11}$ in Fig. 1 and Fig. 2), a pair of cycles $^{1\times4}P_1$(3,0) and $^{1\times4}S_2$(2,1) is born. Here index 1×4 indicates that it is period-4 resonant cycle born on period-1 invariant curve, while subscript index denotes the number index of the bifurcation branch and of the point on the branch. With an increase in the parameter m at $m = 0.1229$, the stable cycle $^{1\times4}P_1$(3,0) undergoes Neimark-Sacker bifurcation (^{4}TR) and transforms into a saddle with a two-dimensional unstable manifold $^{1\times4}S_1$(1,2). The saddle cycle $^{1\times4}S_2$(2,1) for $m = 0.1237$ undergoes a period-doubling bifurcation (^{4}PD$_{11}$), as a result of which it also transforms into a saddle cycle with a two-dimensional unstable manifold $^{1\times4}S_2$(1,2). Then both branches arrive at the point $m = 0.1675$, where they merge as a result of a saddle-node bifurcation (^{4}LP$_{12}$), while cycle $^{1\times4}S_2$(1,2) again undergoes a period-doubling bifurcation (^{4}PD$_{12}$) at $m = 0.1674$ and transforms into $^{1\times4}S_2$(2,1). Continuation of doubled cycles from period-doubling bifurcation points of saddle cycles produces a complex structure in the parameter space - a cascade of doubling of unstable cycles (in Fig. 2a the next two bifurcation points are presented ^{4}PD$_{21}$ and ^{4}PD$_{31}$), which forms a set of branches of saddle cycles with a two-dimensional unstable manifold. It should be noted that with an increase in the parameter m on the Lyapunov exponents chart (Fig. 1) it is clearly seen that soon enough ($m \approx 0.127$) the trajectories begin to run away to infinity, in Fig. 2a this transition is indicated by a red line.

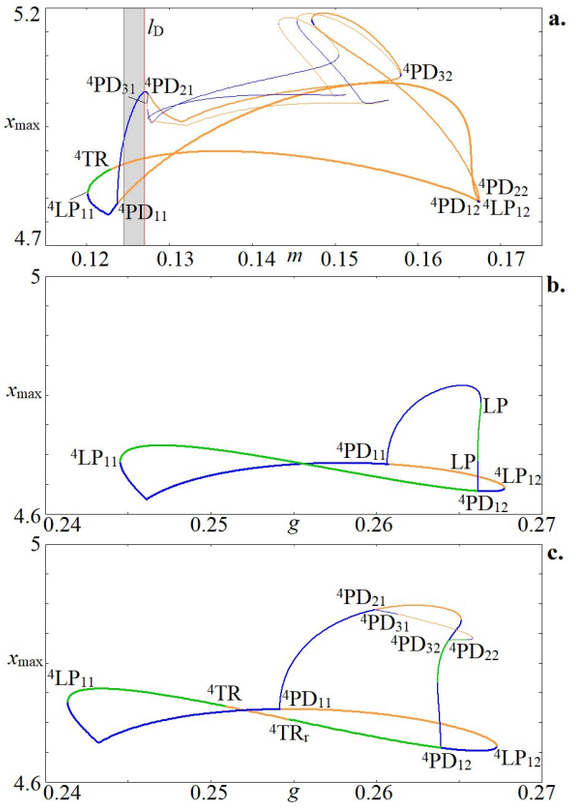

FIG. 2. Bifurcation diagrams for different scan paths across synchronization tongue of period 4, $d = 0.2$, $\gamma = 0.001$. a) $g = 0.236$, b) $m = 0.112$, c) $m = 0.115$. LP are points of the saddle-node bifurcations, PD are points of the period-doubling bifurcations, TR are points of the Neimark-Sacker bifurcation. Red line l_D is threshold of existence stable modes in model (1). Grey color in Fig.2a marks interval corresponding to hyperchaos.

The Fig. 1b shows that the line of period-doubling and Neimark-Sacker bifurcations have a threshold. Hence for small values of the parameter m, there are no bifurcations in which a pair of resonance cycles would be involved. As the parameter m increases, the period-doubling bifurcation line first appears, and then the Neimark-Saker bifurcation line. It is convenient to track the peculiarities of the observed bifurcations by varying the parameter g, since in this case a simpler structure of the parameter space is observed. We will fix two moderate values of the parameter m: $m = 0.112$ and $m = 0.115$, at which we will intersect each of the bifurcation lines, while still not entering the region of strong complication of the diagrams. Figures 2b and 2c show diagrams for $m = 0.112$ and $m = 0.115$, respectively (routes l_2 and l_3 in Fig. 1b).

On the one-parameter continuation diagram at $m = 0.112$, it is clearly seen that on the boundary of the synchronization tongue of period-4, a pair of cycles $^{1\times4}P_1$(3,0) and $^{1\times4}S_2$(2,1) (^{4}LP$_{11}$, g=0.2445) is born. As the parameter g increases, the saddle cycle first undergoes a period-doubling bifurca-

tion (^{4}PD$_{11}$, g = 0.2607), and then the stable cycle (^{4}PD$_{12}$, g = 0.2661) doubles, after which two saddle cycles $^{1\times4}S_1$(2,1) and $^{1\times4}S_2$(1,2) merge at the point of saddle-node bifurcation (^{4}LP$_{12}$, g = 0.2677). The continuation of the cycle from the period-doubling bifurcation point (^{4}PD$_{11}$, g = 0.2607) yields one more bifurcation line, on which two saddle-node bifurcations of the merging of cycles (2,1) and (3,0) are observed, after which the branch of the saddle cycle (2, 1) comes to the period-doubling bifurcation point (^{4}PD$_{12}$, g = 0.2661), which is subcritical. Thus, for small values of the parameter m, the bifurcation diagram mainly demonstrates cycles with a one-dimensional unstable manifold.

As the parameter m increases, this situation changes. Fig. 2c shows a diagram for m = 0.115. In this case, the stable cycle $^{1\times4}P_1$(3,0), born on the boundary of the saddle-node bifurcation (^{4}LP$_{11}$), undergoes a Neimark-Saker bifurcation (^{4}TR), and becomes a saddle type with two-dimensional unstable manifold $^{1\times4}S_1$(1,2), then an inverse Neimark-Sacker bifurcation (^{4}TR$_r$) is observed and the cycle $^{1\times4}S_1$(1,2) is again transformed into $^{1\times4}P_1$(3,0). After that, a period-doubling bifurcation (^{4}PD$_{12}$) occurs with it, and one of the directions of its manifold becomes unstable $^{1\times4}S_1$(2,1). And finally, this cycle at the point of the saddle-node bifurcation (^{4}LP$_{12}$) merges with the cycle $^{1\times4}S_2$(1,2), which in turn appeared as a result of the period-doubling bifurcation (^{4}PD$_{11}$) from the cycle $^{1\times4}S_2$(2,1).

If we build a continuation from the period-doubling points, then a new bifurcation branch appears, which also demonstrates various bifurcations. As a result of doubling (^{4}PD$_{12}$), a doubled cycle $^{1\times4\times2}S_1$(2,1) is born. The cycle $^{1\times4\times2}S_1$(2,1) at the point of the saddle-node bifurcation merges with a new cycle $^{1\times4\times2}P_1$(3,0). With the cycle $^{1\times4\times2}P_1$(3,0) a period-doubling bifurcation (^{4}PD$_{22}$) occurs and it transforms into $^{1\times4\times2}S_2$(2,1), which at the point of the saddle-node bifurcation merges with the cycle $^{1\times4\times2}S_2$(1,2), which also originates from the original bifurcation diagram and undergoes period-doubling. The figure shows a branch coming out of the period-doubling bifurcation point ^{4}PD$_{21}$. Continuation of the cycle born from the third period-doubling bifurcation (^{4}PD$_{31}$) gives similar sequence of bifurcation and new branch of bifurcation diagram with two-dimensional unstable manifold.

To conclude the section, it is clearly seen that with an increase in the parameter m within the basic bifurcation diagram, the dynamics become more complex. In particular, a set of saddle cycles ($^{1\times4}S_2$(1,2), $^{1\times4\times2}S_2$(1,2) and so on) with a two-dimensional unstable manifold is formed via cascade of period-doubling bifurcations of saddle resonance cycle and bifurcation of torus birth of stable cycle. Complicated bifurcation scenarios related to codimension-2 bifurcation points are beyond the scope of the present paper. The aim of this section was to give a sketch of bifurcations forming the period-4 synchronization tongue. Further we will focus on studying the formation of hyperchaotic attractor. The area of interest for us in the parameter space is marked by grey rectangles in Fig. 1b (magnified in Fig. 1c) and in Fig. 2a.

IV. NEIMARK-SACKER BIFURCATION CASCADE IN THE MODIFIED ANISCHENKO-ASTAKHOV GENERATOR

One of the possible paths that the Afraimovich-Shilnikov scenario can take is when the invariant curve loses its smoothness since a pair of multipliers of a stable resonance cycle becomes complex conjugate, and the cycle itself then undergoes a Neimark-Sacker bifurcation with the formation of a new stable invariant curve, which subsequently collapses according to the same scenario, thus forming a cascade of secondary Neimark-Sacker bifurcations. The possibility of the appearance of a cascade of Neimark-Sacker bifurcations of resonance cycles as a result of such a recursive scenario has been known for a long time[18,19]. In the case of three-dimensional systems, new types of attractors do not arise.

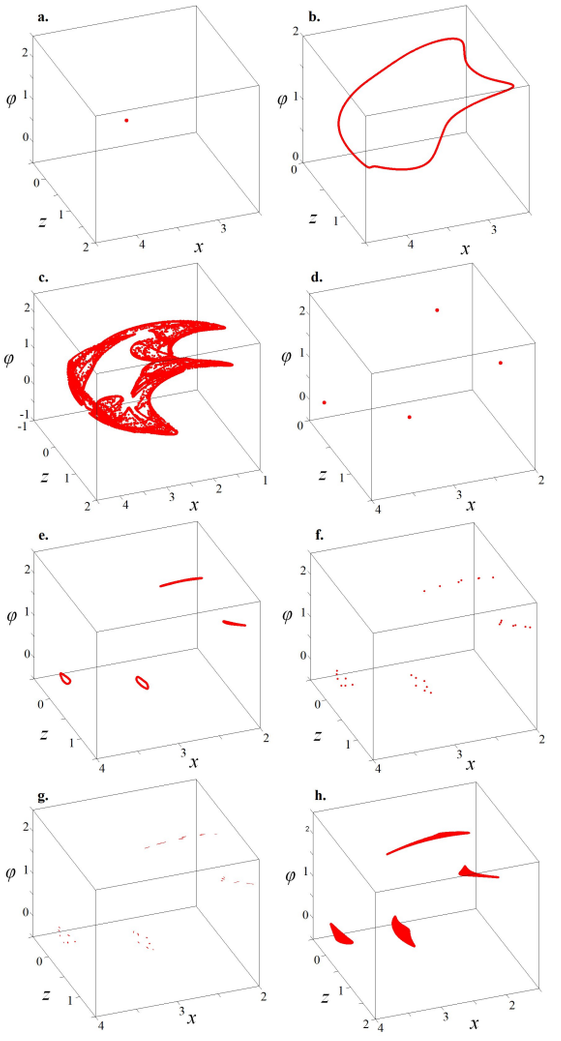

FIG. 3. Phase portraits of the attractors, g=0.236. a) m=0.095 – cycle ^1P; b) m=0.11 – torus ^1T; c) m=0.12 – chaos; d) m=0.122 – resonance cycle $^{1\times4}P$; e) m=0.1235 – torus $^{1\times4}T$; f) m=0.1244 – resonant cycle $^{1\times4\times7}P$; g) m=0.12445 – torus $^{1\times4\times7}T$; h) m=0.125 – hyperchaos $^{1\times4}H$

Systems of higher dimension are another matter. In this case, the appearance of attractors characteristic only for systems of dimension four and higher is possible: - Shilnikov discrete spiral and hyperchaotic. The possibility of the appearance of hyperchaos in systems with secondary Neimark-Sacker bifurcations is discussed in[20–26].

Let us consider the evolution of regimes along the direction $g = 0.236$ (route l_1 in Fig. 1). Fig. 3 shows the phase portraits of attractors for different values of the parameter m in the Poincaré section $y = 0$. First, for small values of m, the system demonstrates a stable ${}^1P$ cycle of period one, Fig. 3a. This cycle undergoes a Neimark-Sacker bifurcation ^{1}TR, turning into a saddle-focus ${}^1S$ of type (1,2), with a two-dimensional unstable manifold and a one-dimensional stable one, while a stable torus ${}^1T$ is born (represented by an invariant circle in Fig. 3b). The torus becomes chaotic with increasing m according to the Afraimovich-Shilnikov scenario (Fig. 3c), and then we find ourselves in the resonance region of period 4 (Fig. 3d). This synchronization tongue reaches here from the ^{1}TR bifurcation line (see Fig. 1). In this region, there is a stable ${}^{1\times4}P$ resonance cycle and a paired ${}^{1\times4}S$ saddle cycle of period 4. The stable cycle, in turn, loses its stability via the Neimark-Saker bifurcation (^{4}TR) with the formation of a stable ${}^{1\times4}T$ torus (invariant circle of period 4 in Fig. 3e) and a ${}^{1\times4}S$ saddle-focus of type (1, 2). This torus also chaotizes, followed by a region of resonance of period 28 with cycles ${}^{1\times4\times7}P$ and ${}^{1\times4\times7}S$, followed by a region of existence of the torus ${}^{1\times4\times7}T$, and so on. Fig. 4 shows a phase portrait of a torus ${}^{1\times4\times7\times9\times9\times10}T$ in the Poincaré section.

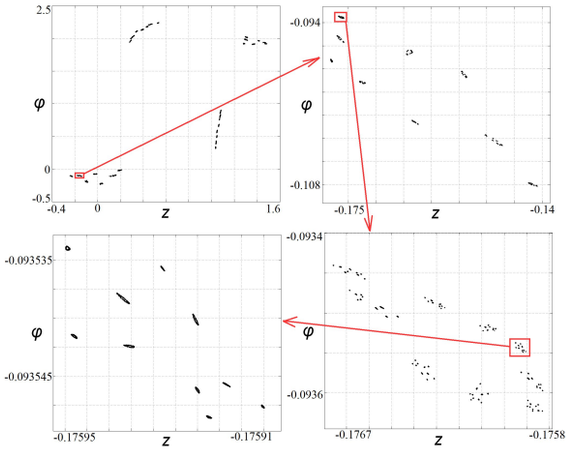

FIG. 4. Phase portrait of the torus attractor ${}^{1\times4\times7\times9\times9\times10}T$, m=0.124457208289, $g = 0.236$, $d = 0.2$, $\gamma = 0.001$.

This entire cascade accumulates near the threshold of hyperchaos. Fig. 5a shows a graph of the dependence of the two largest Lyapunov exponents (excluding the trivial zero one) on the parameter m. Figures 5b, 5c, 5d, 5e show successive enlarged fragments of these graphs in the immediate vicinity of the point at which the hyperchaos occurs. The plots show the points of the Neimark-Sacker bifurcations TR of the resonance cycles. As a result of the cascade of Neimark-Sacker bifurcations, there is a hierarchy of saddle-focus cycles at the accumulation point. The inverse cascade of absorption by the attractor of a set of these cycles with a two-dimensional unstable manifold leads to the fact that the attractor formed behind the accumulation point turns out to be hyperchaotic; it will be shown in Section VI.

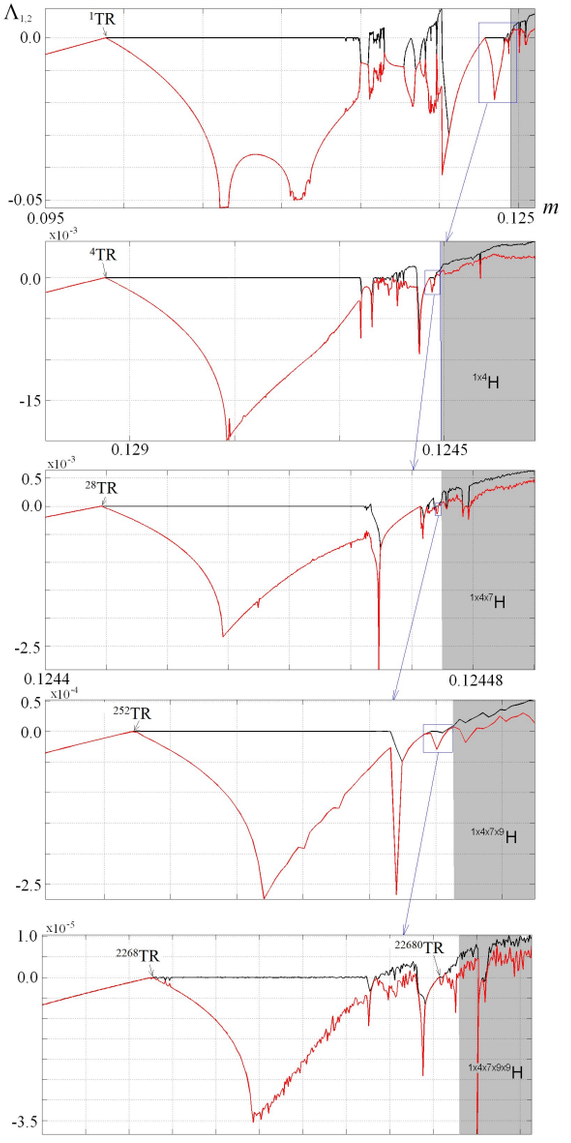

FIG. 5. Graphs of the two largest Lyapunov exponents with a sequential magnification in the vicinity of the hyperchaos threshold. The points of Neimark-Sacker bifurcations TR of resonance cycles and the regions of existence of hyperchaotic attractors of various periods are indicated. $g = 0.236$, $d = 0.2$, $\gamma = 0.001$.

V. CASCADES OF PERIOD-DOUBLING BIFURCATIONS OF SADDLE RESONANCE CYCLES

As was mentioned in Sect. III, in parallel to the above-described cascade of Neimark-Sacker bifurcations of stable

resonance cycles, the evolution of unstable resonance cycles develops. Each of them undergoes a cascade of period-doubling bifurcations, as a result of which a saddle hyperchaotic set arises in the phase space. Tables II and III show the bifurcation values of the parameter m for the first steps of the cascade for unstable cycles ${}^{1\times4\times7}S$ and ${}^{1\times4\times7\times9}S$.

Cycle period	m
28	0.124370616
56	0.124427167
112	0.124450152
224	0.124455662

TABLE II. Bifurcation values of the parameter m for the first steps of the cascade for unstable cycle ${}^{1\times4\times7}S$.

Cycle period	m
252	0.1244564989
504	0.1244571880
1008	0.1244574263

TABLE III. Bifurcation values of the parameter m for the first steps of the cascade for unstable cycle ${}^{1\times4\times7\times9}S$.

VI. INVERSE CASCADE OF DISCRETE SPIRAL HYPERCHAOTIC ATTRACTORS MERGING

As a result of the cascade of Neimark-Sacker bifurcations, there is a hierarchy of saddle-focus cycles $S(1,2)$ at the accumulation point, as well as dual sequence of saddle hyperchaotic sets. The inverse cascade of absorption by the attractor of the set of these cycles possessing a two-dimensional unstable manifold leads to the fact that the attractor formed behind the accumulation point turns out to be hyperchaotic

In Fig. 5 gray color indicates the regions of existence of hyperchaotic attractors H arising at successive stages of development of the inverse absorption cascade of saddle-focus cycles $S(1,2)$.

As a typical in the case under study phase portrait of a hyperchaotic attractor, Fig. 6a shows an attractor ${}^{1\times4\times7\times9}H$ (only a part of the attractor is shown; i. e. only every 28th iteration is displayed). In the following pictures, Fig. 6 illustrates the process of transformation of the attractor ${}^{1\times4\times7\times9}H$ into the attractor ${}^{1\times4\times7}H$. In Fig. 6a, besides the attractor, crosses indicate the elements of several cycles from those that constitute the saddle hyperchaotic set arising as a result of the period-doubling cascade of the unstable resonance cycle ${}^{1\times4\times7\times9}S$. First, the attractor absorbs cycles from this hyperchaotic set, while the individual elements of the ${}^{1\times4\times7\times9}H$ attractor are combined into a ring with a "hole" in the middle, in which the element of the saddle-focus cycle ${}^{1\times4\times7}S$ is located, Fig. 6b. Then, in accordance with the scenarios proposed in[12,13], it becomes possible for the attractor to absorb the saddle-focus cycle ${}^{1\times4\times7}S$ with the emergence of a homoclinic bifurcation of the closure of the stable and unstable manifold of this cycle. This gives rise to discrete spiral Shilnikov attractor. In Fig. 6c, it can be seen that the attractor covers its entire inner region.

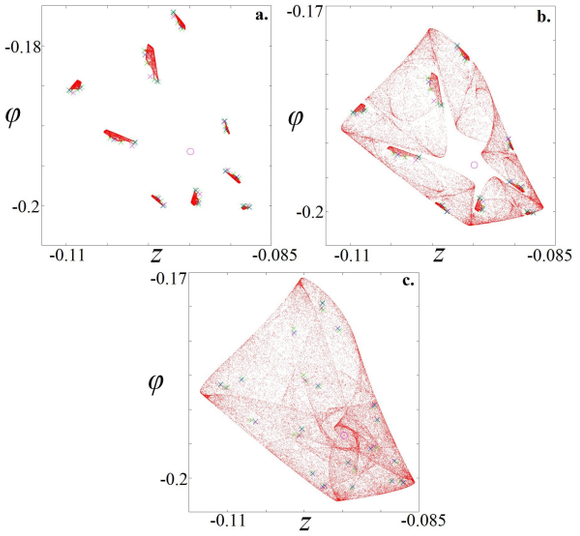

FIG. 6. Transformation of the attractor from the 252-component hyperchaotic ${}^{1\times4\times7\times9}H$ into the 28-component hyperchaotic ${}^{1\times4\times7}H$ in the supercritical region; a) $m = 0.124457465$; b) $m = 0.12445748$; c) $m = 0.1244620$. The crosses indicate the cycles included in the saddle hyperchaotic set, purple - period 252, blue - 504, green - 1008. The purple circle in the center indicates the saddle-focus of period 28.

VII. DISCUSSION

Due to its limitations, numerical analysis cannot give an answer to the question of the finiteness or infinitness of the cascade of Neimark-Sacker bifurcations on the border of the origin of hyperchaos. Nevertheless, it may be suggested that attractor eventually chaotizes in some way, for example via period-doubling scenario, and then experiences the transition from chaos to hyperchaos by absorbing the cycles which arise along with the cascade of Neimark-Sacker bifurcations. The paper[26] points out the role that the absorbing the saddle-focus cycles and emergence of a discrete spiral Shilnikov attractor play in the formation of a hyperchaotic attractor. However, absorbing only finite number of saddle-focus cycles seems insufficient for the attractor to became hyperchaotic, it requires the absorption of an infinite number of orbits with two-dimensional unstable manifold[2–4]. We show here the way the needed cycles may be emerged via the period doubling cascades of unstable cycles.

In this paper, we propose a mechanism for the emergence of a hyperchaotic attractor in systems with a secondary Neimark-Sacker bifurcation in synchronization tongues. The existence of a cascade of Neimark-Sacker bifurcations at the threshold of the appearance of hyperchaos and an inverse cascade of absorption bifurcations of a set of saddle-focus cycles and hyperchaotic saddle sets arising as a result of cascades of period-

doubling bifurcations of saddle resonance cycles is demonstrated. It can be assumed that this mechanism is quite general and manifests itself in systems of a very different nature[20–26].

ACKNOWLEDGMENTS

The work of I.R.Sataev was carried out within the framework of the state task of Kotel'nikov IRE RAS. The work of N.V.Stankevich was carried out within the grant RFBR (project No. 19-31-60030) and partially supported by Laboratory of Dynamical Systems and Applications NRU HSE, of the Ministry of science and higher education of the RF grant ag. No 075-15-2019-1931. We also wish to acknowledge Kazakov A.O. for useful discussions and suggestions.

DATA AVAILABILITY

The data supporting numerical experiments presented in this paper are available from the corresponding author upon reasonable request.

[1]O. Rossler, "An equation for hyperchaos," Physics Letters A **71**, 155–157 (1979).
[2]T. Kapitaniak, Y. Maistrenko, and S. Popovych, "Chaos-hyperchaos transition," Physical Review E **62**, 1972 (2000).
[3]T. Kapitaniak, K.-E. Thylwe, I. Cohen, and J. Wojewoda, "Chaos-hyperchaos transition," Chaos, Solitons & Fractals **5**, 2003–2011 (1995).
[4]S. Yanchuk and T. Kapitaniak, "Symmetry-increasing bifurcation as a predictor of a chaos-hyperchaos transition in coupled systems," Physical Review E **64**, 056235 (2001).
[5]M. A. Harrison and Y.-C. Lai, "Route to high-dimensional chaos," Physical Review E **59**, R3799 (1999).
[6]S. Nikolov and S. Clodong, "Hyperchaos–chaos–hyperchaos transition in modified rössler systems," Chaos, solitons & fractals **28**, 252–263 (2006).
[7]K. Harikrishnan, R. Misra, and G. Ambika, "On the transition to hyperchaos and the structure of hyperchaotic attractors," The European Physical Journal B **86**, 394 (2013).
[8]Q. Li, S. Tang, and X.-S. Yang, "Hyperchaotic set in continuous chaos–hyperchaos transition," Communications in Nonlinear Science and Numerical Simulation **19**, 3718–3734 (2014).
[9]L. Munteanu, C. Brişan, V. Chiroiu, D. Dumitriu, and R. Ioan, "Chaos–hyperchaos transition in a class of models governed by sommerfeld effect," Nonlinear Dynamics **78**, 1877–1889 (2014).
[10]L. Shilnikov, "Theory of bifurcations and turbulence. i," in *In Collection "Methods of qualitative theory of differential equations"* (Gorky, 1986) pp. 150–165.
[11]L. Shilnikov, "Theory of bifurcations and turbulence. i," in *Selecta Mathematica Sovietica*, Vol. 10 (1991) pp. 43–53.
[12]A. Gonchenko, S. Gonchenko, A. Kazakov, and D. Turaev, "Simple scenarios of onset of chaos in three-dimensional maps," International Journal of Bifurcation and Chaos **24**, 1440005 (2014).
[13]A. Gonchenko, S. Gonchenko, and L. Shilnikov, "Towards scenarios of chaos appearance in three-dimensional maps," Rus. J. Nonlin. Dyn **8**, 3–28 (2012).
[14]V. Anishchenko and S. Nikolaev, "Generator of quasi-periodic oscillations featuring two-dimensional torus doubling bifurcations," Technical physics letters **31**, 853–855 (2005).
[15]V. Anishchenko, S. Nikolaev, and J. Kurths, "Peculiarities of synchronization of a resonant limit cycle on a two-dimensional torus," Physical Review E **76**, 046216 (2007).
[16]B. Ermentrout, *Simulating, analyzing, and animating dynamical systems: a guide to XPPAUT for researchers and students* (SIAM, 2002).
[17]V. Afraimovich and L. P. Shilnikov, "Invariant two-dimensional tori, their breakdown and stochasticity," Amer. Math. Soc. Transl **149**, 201–212 (1991).
[18]V. Anishchenko, T. Letchford, and M. Safonova, "Phase-locking effects and bifurcations of phase-locked and quasi-periodic oscillations in a nonautonomous oscillator," RaF **28**, 1112–1125 (1985).
[19]A. Kipchatov and A. Koronovsky, "Fine effects of self-similar behavior of a piecewise-linear system near the bifurcation line of torus birth," Izvestiya VUZ, Appl. Nonlin. Dyn **5**, 17–23 (1997).
[20]N. V. Stankevich, A. Dvorak, V. Astakhov, P. Jaros, M. Kapitaniak, P. Perlikowski, and T. Kapitaniak, "Chaos and hyperchaos in coupled antiphase driven toda oscillators," Regular and Chaotic Dynamics **23**, 120–126 (2018).
[21]A. Kuznetsov and Y. V. Sedova, "Coupled systems with hyperchaos and quasiperiodicity," Journal of Applied Nonlinear Dynamics **5**, 161–167 (2016).
[22]P. C. Rech, "Hyperchaos and quasiperiodicity from a four-dimensional system based on the lorenz system," The European Physical Journal B **90**, 251 (2017).
[23]T. F. Fonzin, J. Kengne, and F. Pelap, "Dynamical analysis and multistability in autonomous hyperchaotic oscillator with experimental verification," Nonlinear Dynamics **93**, 653–669 (2018).
[24]N. Stankevich, A. Kuznetsov, E. Popova, and E. Seleznev, "Chaos and hyperchaos via secondary neimark–sacker bifurcation in a model of radiophysical generator," Nonlinear dynamics **97**, 2355–2370 (2019).
[25]N. Stankevich and E. Volkov, "Evolution of quasiperiodicity in quorum-sensing coupled identical repressilators," Chaos: An Interdisciplinary Journal of Nonlinear Science **30**, 043122 (2020).
[26]I. R. Garashchuk, D. I. Sinelshchikov, A. O. Kazakov, and N. A. Kudryashov, "Hyperchaos and multistability in the model of two interacting microbubble contrast agents," Chaos: An Interdisciplinary Journal of Nonlinear Science **29**, 063131 (2019).
[27]Y. A. Kuznetsov, H. G. Meijer, and L. van Veen, "The fold-flip bifurcation," International Journal of Bifurcation and Chaos **14**, 2253–2282 (2004).

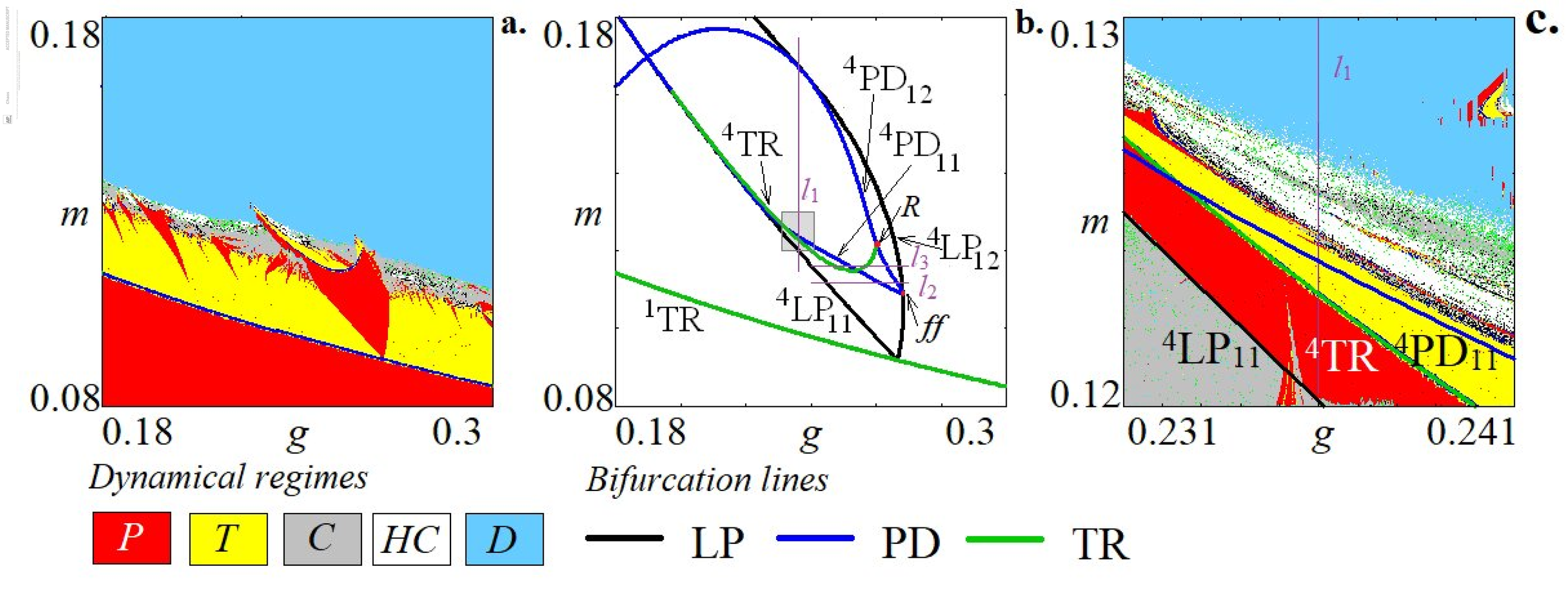
a.
b.
c.
0.18
0.08
m
0.18
g
0.3
Dynamical regimes
P
T
C
HC
D
Bifurcation lines
$^4PD_{12}$
$^4PD_{11}$
^4TR
l_1
R
$^4LP_{12}$
l_3
l_2
ff
$^4LP_{11}$
^1TR
LP
PD
TR
0.13
0.12
0.231
0.241